

THE RADIATIVE $^{10}\text{Be}(n,\gamma)^{11}\text{Be}$ CAPTURE AT THERMAL AND ASTROPHYSICAL ENERGIES

Dubovichenko S.B.,¹ Dzhazairov-Kakhramanov A.V.²

V.G. Fessenkov Astrophysical Institute, National Center of Space Research and Technologies, ASC MID RK, Almaty, Kazakhstan

¹dubovichenko@mail.ru, ²albert-j@yandex.ru

Abstract

Within the framework of the modified potential cluster model with the forbidden states and the classification of states according to Young tableaux the possibility of describing the available experimental data for the total reaction cross sections of the neutron radiative capture on ^{10}Be at thermal and astrophysical energies was shown.

1. Introduction

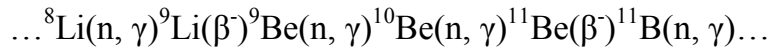
In the middle of nineties in papers [1,2] the possibility of describing the Coulomb form factors of $^{6,7}\text{Li}$, having a high degree of clusterization in the two-body channels, based on the single-channel two-body potential cluster model (PCM) was demonstrated [3-5]. This variant of the model is based on the concept of forbidden states (FSs) [4-9] in the intercluster potentials. The presence of the FSs leads to the appearance of "extra" nodes in the wave functions (WFs) of the relative cluster motion. The forbidden states were used by us more in papers [10,11], the consideration of which in a simple PCM allowed one to get an acceptable description of the main characteristics of some light nuclei. Furthermore, in the PCM with the consideration of tensor forces [12,13], the possibility of a correct reproduction of almost all main characteristics of ^{6}Li was demonstrated, including the well-known, at that time, the value of its quadrupole moment.

Furthermore, in papers [3-5,14-33] the possibility of an acceptable description of the known experimental data on the astrophysical S -factors or the total cross sections for radiative capture on some light nuclei was demonstrated. Namely, the capture in systems $p^2\text{H}$, $n^2\text{H}$, $p^3\text{H}$, $p^6\text{Li}$, $n^6\text{Li}$, $p^7\text{Li}$, $n^7\text{Li}$, $n^8\text{Li}$, $p^9\text{Be}$, $n^9\text{Be}$, $p^{10}\text{B}$, $n^{10}\text{B}$, $p^{11}\text{B}$, $n^{11}\text{B}$, $p^{12}\text{C}$, $n^{12}\text{C}$, $p^{13}\text{C}$, $n^{13}\text{C}$, $p^{14}\text{C}$, $n^{14}\text{C}$, $n^{14}\text{N}$, $p^{15}\text{N}$, $n^{15}\text{N}$, $n^{16}\text{O}$ and $^2\text{H}^4\text{He}$, $^3\text{He}^4\text{He}$, $^3\text{H}^4\text{He}$, $^4\text{He}^{12}\text{C}$ at thermal and astrophysical energies was considered. The calculations of these capture processes are based on a modified version of PCM with the FSs and the classification of cluster states according to Young tableaux (MPCM), the methods of which were described in details in papers [26-33] and [34].

This quite remarkable success of the MPCM can be explained by the fact that the potentials of intercluster interaction in the continuous spectrum are constructed not only on the basis of the known elastic scattering phase shifts, but also taking into account the classification of cluster states according to Young tableaux [35]. The potential parameters of the bound states (BSs) at a given number of the allowed states (ASs) and forbidden states in the given partial wave are also fixed quite clearly. For this purpose, for instance, the requirement of description of the nucleus binding energy in the cluster channel and its charge radius and two-body asymptotic constant (AC) is used [34]. Furthermore, such potentials allow one to perform the calculations, for example, of the

astrophysical S -factors of the radiative capture reactions [36] or the total cross sections of these reactions [37] at low and ultralow energies. These calculations include, in some cases the thermal energy range and as a whole allow to reproduce the available experimental data for the total cross sections of the capture reactions and some characteristics of the BSs for the most considered light nuclei [3,34].

Continuing the study of radiative capture processes [3,34], let's consider the reaction $n+^{10}\text{Be} \rightarrow ^{11}\text{Be}+\gamma$ in the frame of the MPCM at thermal and astrophysical energies. This reaction is a part of one of the variant of the chain of primordial nucleosynthesis of the Universe [38]



by which the elements with a mass of $A > 11-12$ can be formed (see., e.g., [39]).

2. The structure of the $n^{10}\text{Be}$ states

For ^{10}Be , as well as for ^{10}B [34], we accept the Young tableau $\{442\}$, therefore for the $n^{10}\text{Be}$ system we have $\{1\} \times \{442\} \rightarrow \{542\} + \{443\} + \{4421\}$ [35,40]. The first from the obtained tableaux compatible with the orbital angular moments $L = 0, 2, 3, 4$, and is forbidden because it is forbidden to have more than four nucleons in the s -shell, the second tableau is allowed and compatible with the orbital angular moments $L = 1, 2, 3, 4$, and the third is also allowed, compatible with $L = 1, 2, 3$ [35].

Generally speaking, the lack of the tables of products of the Young tableaux for the number of particles 10 and 11 makes it impossible to make an accurate classification of the cluster states in the given system of particles. However, even such a qualitative estimation of orbital symmetries allows one to determine the presence of the FSs in the S wave and lack of the FSs for the P states. Exactly such structure of the FSs and ASs in the different partial waves allows to build further the potentials of intercluster interaction, which are necessary for the calculation of the total cross sections for the considering radiative capture reaction [3,34].

Thus, taking into account only the lower partial waves with orbital angular moments $L = 0, 1, 2$, it can be said that for the $n^{10}\text{Be}$ system (for $^{10}\text{Be} J^\pi, T = 0^+, 1$ [41]) in the potentials of the 2P waves only the allowed state presents, and 2S and 2D waves have the forbidden states. The state in the ${}^2S_{1/2}$ wave (in the notation of ${}^{(2S+1)}L_J$), corresponds to the GS of ^{11}Be with $J^\pi, T = 1/2^+, 3/2$ and is located at the binding energy of the $n^{10}\text{B}$ system of -0.5016 MeV [42].

Note that the 2P waves correspond to the two allowed Young tableaux $\{443\}$ and $\{4421\}$. This situation seems to be similar to the systems N^2H or N^{10}B , described in [3,14,28-31,34], where the potentials for the scattering processes depend on two Young tableaux, and for the BS only on one [43,44]. Therefore, here we assume that the potential ${}^2P_{1/2}$ of the BS (first excited state – FES) corresponds to one tableau $\{443\}$. Consequently, the potentials of the ${}^2P_{1/2}$ BS and of the ${}^2P_{1/2}$ scattering processes are different, because they depend on a different set of Young tableaux. To fix the idea we will assume that for a discrete spectrum the allowed state in the ${}^2P_{1/2}$ wave is bound, while for the scattering processes it is not bound. Therefore, the depth of such

potential can be simply set equal to zero. The FS occurs to be the bound state for the ${}^2S_{1/2}$ scattering wave or for the discrete spectrum in the $n^{10}\text{B}$ system.

Now let us consider the FES, bound in the $n^{10}\text{Be}$ channel, and the first resonance state (FRS) of ${}^{11}\text{Be}$ [42], which is not bound in the $n^{10}\text{Be}$ channel and corresponds to the resonance in the $n^{10}\text{Be}$ scattering. The FES of ${}^{11}\text{Be}$ is located at energy of 0.32004 MeV comparatively to the GS with the $J^\pi = 1/2$ moment or -0.18156 MeV comparatively to the $n^{10}\text{Be}$ channel threshold. This state can be related to the doublet ${}^2P_{1/2}$ level without FS. The first resonance state is located at 1.783 MeV comparatively to the GS or at 1.2814 MeV comparatively to the $n^{10}\text{Be}$ channel threshold. For this level the moment $J^\pi = 5/2^+$ [42] is provided, which allows to take $L = 2$ for it, i.e., to consider it as the ${}^2D_{5/2}$ resonance in the $n^{10}\text{Be}$ system at 1.41 MeV in the laboratory system (l.s.), and its potential has the FS. The width of such resonance is equal to 100(10) keV in the center of mass (c.m.) [42].

On the basis of these data, it is reputed that the $E1$ capture from the 2P scattering waves with the potential of zero depth without the FSs to the ${}^2S_{1/2}$ GS of ${}^{11}\text{Be}$ with the bound FS is possible.

$$\text{No. 1. } \begin{array}{l} {}^2P_{1/2} \rightarrow {}^2S_{1/2} \\ {}^2P_{3/2} \rightarrow {}^2S_{1/2} \end{array} .$$

For the radiative capture to the FES the similar $E1$ transition from the ${}^2S_{1/2}$ and ${}^2D_{3/2}$ scattering waves with the bound FSs to the ${}^2P_{1/2}$ BS without FS is possible.

$$\text{No. 2. } \begin{array}{l} {}^2S_{1/2} \rightarrow {}^2P_{1/2} \\ {}^2D_{3/2} \rightarrow {}^2P_{1/2} \end{array} .$$

The GS potentials and the FES will be constructed further in a way for correct description of the channel binding energy, the charge radius of ${}^{11}\text{Be}$ and its asymptotic constant in the $n^{10}\text{Be}$ channel. Therefore, the known values of the asymptotic normalization coefficient (ANC) and the spectroscopic factor S , with help of which the AC is found, have a quite big error, the GS potentials will also have several variants with different parameters of width, which strongly affect the value of the AC.

The data on the asymptotic normalization coefficients A_{NC} , for example, are given in paper [48]. Here we will also use the well-known relation

$$A_{NC}^2 = S \times C^2, \quad (1)$$

where S – the spectroscopic factor, C – asymptotic constant in $\text{fm}^{-1/2}$, which is connected with the dimensionless AC [45] C_w , used by us as follows: $C = \sqrt{2k_0} C_w$, and the dimensionless constant C_w is given by the expression [45]

$$\chi_L(r) = \sqrt{2k_0} C_w W_{-\eta L + 1/2}(2k_0 r), \quad (2)$$

where $\chi_L(r)$ – numerical wave function of the bound state, obtained from the solution of the radial Schrödinger equation and normalized to unity, $W_{-\eta L+1/2}$ – the Whittaker function of the bound state, which determines the asymptotic behavior of the wave function and is a solution of the same equation without nuclear potential, k_0 – the wave number caused by the E channel energy $k_0 = \sqrt{2\mu \frac{m_0}{\hbar^2} E}$, η – the Coulomb parameter $\eta = \frac{\mu Z_1 Z_2 e^2}{\hbar^2 k}$, determined numerically $\eta = 3.44476 \cdot 10^{-2} \frac{\mu Z_1 Z_2}{k}$ and L – the orbital angular momentum of the bound state. Here μ – the reduced mass of particles of the input channel, and the constant \hbar^2 / m_0 was assumed equal to 41.4686 fm², where m_0 is the atomic mass unit (amu).

In further calculations we used the radius of ¹⁰Be in the GS equals 2.357(18) fm from paper [46], and for the GS of ¹¹Be the known radius value of 2.463(15) fm is given in [42]. The charge radius of the neutron assumed to be zero, and its massive range 0.8775(51) fm coincides with the known radius of the proton [50]. In addition, for the charge radius of the FES of ¹¹Be the calculated value of 2.43(10) fm [47] is known, and for the GS the value 2.42(10) fm is obtained in the same paper. For the radius of the neutron in ¹¹Be estimation equals 5.6(6) fm is given [47]. At the same time in paper [48] for the neutron radius in the GS the value of 7.60(25) fm is given, while for the FES of -4.58(25) fm. In the all calculations for the masses of nucleus and neutron the exact values are used: $m(^{10}\text{Be}) = 10.013533$ amu [49] and $m(n) = 1.00866491597$ amu [50].

3. Methods for calculating of the total cross sections

The total cross sections of the radiative capture $\sigma(NJ, J_f)$ for the EJ transitions in the potential cluster model are given, for example, in [3,28-31,34] or [36] and have the form

$$\sigma_c(NJ, J_f) = \frac{8\pi K e^2}{\hbar^2 q^3} \frac{\mu}{(2S_1 + 1)(2S_2 + 1)} \frac{J + 1}{J[(2J + 1)!!]^2} A_J^2(NJ, K) \cdot \sum_{L_i, J_i} P_J^2(NJ, J_f, J_i) I_J^2(J_f, J_i),$$

where σ – the total cross section of the process of the radiative capture, μ – the reduced mass of particles of the input channel, q – the wave number of particles of the input channels, S_1, S_2 – spins of the particles in the input channel, K, J – the wave number and the moment of γ quantum in the output channel, N – it is the E or M transitions of J -th multipolarity from the initial state J_i to the final state J_f of the nucleus.

For the electric orbital $EJ(L)$ transitions ($S_i = S_f = S$) the value P_J has the form [3,34]

$$P_J^2(EJ, J_f, J_i) = \delta_{S_i S_f} [(2J+1)(2L_i+1)(2J_i+1)(2J_f+1)] (L_i 0 J 0 | L_f 0)^2 \left\{ \begin{matrix} L_i & S & J_i \\ J_f & J & L_f \end{matrix} \right\}^2$$

$$A_J(EJ, K) = K^J \mu^J \left(\frac{Z_1}{m_1^J} + (-1)^J \frac{Z_2}{m_2^J} \right), \quad I_J(J_f, J_i) = \langle \chi_f | R^J | \chi_i \rangle \quad (3)$$

Here $S_i, S_f, L_i, L_f, J_i, J_f$ are the total spins and moments of particles in the input (i) and the output (f) channel; μ, m_1, m_2, Z_1, Z_2 are the reduced mass, the masses and the charges of particles in the input channel; I_J is the integral over the wave functions of the initial χ_i and final χ_f state as the functions of the relative motion of clusters, in this case, the neutron and ${}^8\text{Li}$, with the interparticle distance R .

For the spin part of the magnetic process $M1(S)$ in the MPCM the following expression is used ($S_i = S_f = S, L_i = L_f = L$) [34]:

$$P_1^2(M1, J_f, J_i) = \delta_{S_i S_f} \delta_{L_i L_f} [S(S+1)(2S+1)(2J_i+1)(2J_f+1)] \left\{ \begin{matrix} S & L & J_i \\ J_f & 1 & S \end{matrix} \right\}^2$$

$$A_1(M1, K) = i \frac{\hbar K}{m_0 c} \sqrt{3} \left[\mu_1 \frac{m_2}{m} - \mu_2 \frac{m_1}{m} \right], \quad I_1(J_f, J_i) = \langle \chi_f | R^{J-1} | \chi_i \rangle, \quad J=1. \quad (4)$$

Here m – mass of the nucleus, μ_1, μ_2 – the magnetic moments of the clusters, the other symbols are the same as in the previous terms. For the neutron magnetic moment and ${}^{10}\text{Be}$ the following values were used: $\mu_n = -1.91304272\mu_0$ and $\mu({}^{10}\text{Be}) = 0$ [41], where μ_0 – nuclear magneton. The correctness of the above expression for the $M1$ transition pre-tested in our previous papers [3,14,17,34] on the basis of neutron radiative capture on ${}^7\text{Li}$ and proton radiative capture on ${}^2\text{H}$ reactions at low and astrophysical energies.

4. The $n^{10}\text{Be}$ interaction potentials

As usual [3,14-17,26-31,34], in the capacity of the $n^{10}\text{Be}$ interaction in each partial wave with a given orbital angular moment L we use the potential of the Gaussian form with the point-like Coulomb term

$$V(r, L) = -V_L \exp(-\gamma_L r^2). \quad (5)$$

The ground state of ${}^{11}\text{Be}$ in the $n^{10}\text{Be}$ channel is the ${}^2S_{1/2}$ level and this potential should describe the AC of this channel correctly. In order to extract this constant from the available experimental data, let us consider information about the spectroscopic factor S and the asymptotic normalization coefficients A_{NC} . The results for A_{NC} are given in paper [48] that are presented in Table 1, here some results from paper [38] are added. In addition to this, a relatively large amount of data for the spectroscopic

factors of the $n^{10}\text{Be}$ channel of ^{11}Be is managed to find [42], so we give their values in the separate Table 2.

Table 1. The A_{NC} data of ^{11}Be in the $n^{10}\text{Be}$ channel

Reaction from which the A_{NC} is determined	The value of the A_{NC} in $\text{fm}^{-1/2}$ for the GS	The value of the A_{NC} in $\text{fm}^{-1/2}$ for the FES	Literature
(d,p_0) at 12 MeV	0.723(16)	0.133(4)	[48]
(d,p_0) at 25 MeV	0.715(35)	0.128(6)	[48]
(d,p_0) at 25 MeV	0.81(5)	0.18(1)	[38]
	<i>0.68–0.86</i>	<i>0.122–0.19</i>	<i>Interval</i>
	<i>0.749</i>	<i>0.147</i>	Average \bar{A}_{NC}

Furthermore, based on the expression (1) for the GS we find $\bar{A}_{NC}/\sqrt{\bar{S}} = \bar{C} = 0.94 \text{ fm}^{-1/2}$, and since $\sqrt{2k_0} = 0.546$, then the dimensionless AC defined as $\bar{C}_w = \bar{C}/\sqrt{2k_0}$, is equal to $\bar{C}_w = 1.72$. However, the range of values of the spectroscopic factor is so high that the value C_w may be in the range of 1.54-2.29, and if we consider the errors of A_{NC} , then this interval can be extended to 1.40-2.63. For the FES at $\sqrt{2k_0} = 0.423$ we find $\bar{C}_w = 0.45$ similarly, and the range of values \bar{C}_w for the average ANC is equal to 0.35-0.62. If we consider the A_{NC} errors, then this interval is expanded to 0.29-0.81.

Table 2. Data for the spectroscopic factors S of ^{11}Be in the $n^{10}\text{Be}$ channel

The S value for the GS	The S value for the FES	Literature
0.42(6)	0.37(6)	[51]
0.72(4)	---	[52]
0.61(5)	---	[53]
0.56(18)	0.44(8)	[54,55]
0.73(6)	0.63(15)	[56,57]
0.77	0.96	[58]
<i>0.36–0.79</i>	<i>0.31–0.96</i>	<i>Interval</i>
<i>0.64</i>	<i>0.6</i>	Average \bar{S}

The potential ${}^2S_{1/2}$ of the GS with the FS, which allows one to get the dimensionless constant C_w , close to the average value of 1.72, has the parameters

$$V_{1/2} = 47.153189 \text{ MeV and } \gamma_{1/2} = 0.1 \text{ fm}^{-2}. \quad (6)$$

It leads to the binding energy of -0.501600 MeV with an accuracy of the used herein finite-difference method (FDM) for the calculating of the binding energy of 10^{-6} MeV [7], the AC $C_w = 1.73(1)$ on the interval of 7-30 fm, the mass radius of 3.16 fm,

the charge radius of 2.46 fm. The determination of the estimated expressions of these radiuses is given, for example, in papers [1-3,34]. The AC errors are determined by its averaging over the specified range of distances.

Such potential of the GS with the FS is in a full accordance with the classification of states according to Young tableaux given above, and gives the charge radius of ^{11}Be which is in a good agreement with data [42]. The parameters of the GS potential were constructed on the basis of the approximate description of the average value of the AC equals 1.72 received above, and its phase shift that shown in figure 1 by the solid line. This potential at the orbital angular momentum $L = 2$ leads to the non-resonant 2D scattering phase shift without spin-orbital splitting shown in figure 1 by the dotted line. On the same figure the $^2S_{1/2}$ phase shifts of the $n^{10}\text{Be}$ scattering, obtained in the calculations in work [59], are shown by points.

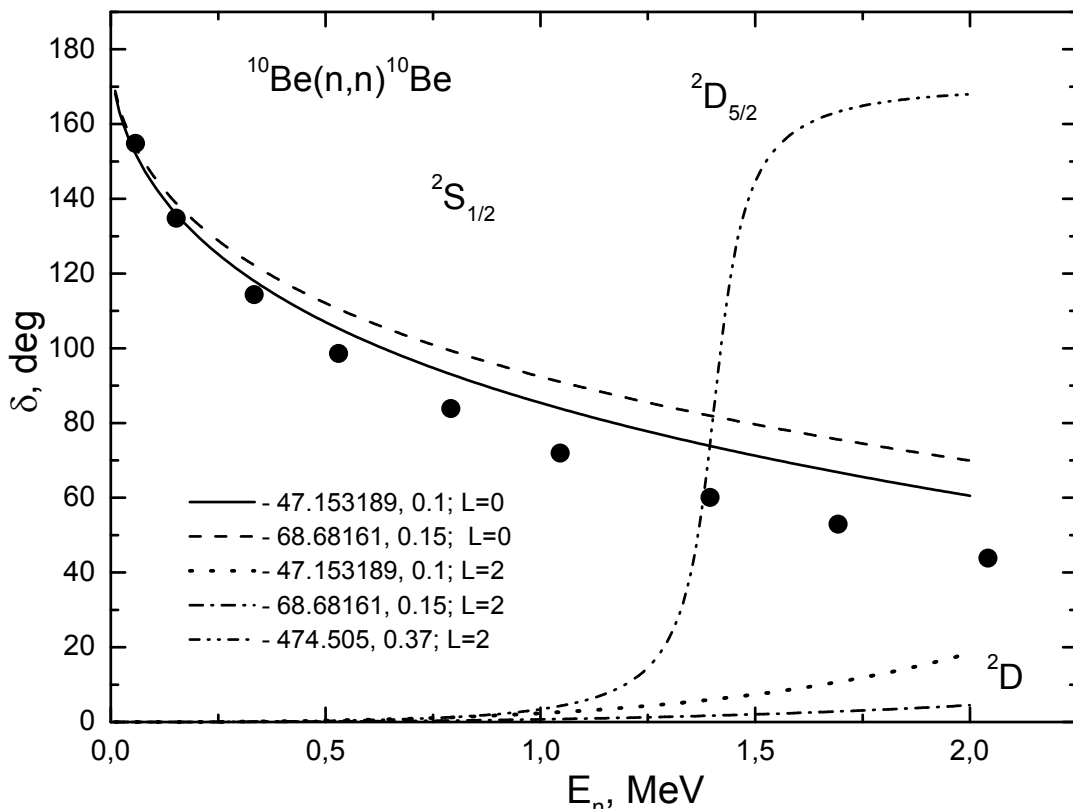


Figure 1. The $n^{10}\text{Be}$ elastic scattering phase shifts of the $^2S_{1/2}$ wave. The meaning of the lines and points is explained in the text.

To compare the results, let us consider another variant of the potential of the GS with the FS and the parameters

$$V_{1/2} = 68.68161 \text{ MeV and } \gamma_{1/2} = 0.15 \text{ fm}^2. \quad (7)$$

The potential leads to the binding energy of -0.501600 MeV at the same accuracy of the FDM, $C_W = 1.56$ (1) on the interval of 5–30 fm, the mass radius of 3.05 fm, the charge radius of 2.45 fm and its phase shift is shown in figure 1 by the dashed line. The dimensionless AC is close to the lower limit of the range of values of this magnitude 1.54–2.29. Such potential with the orbital angular momentum $L = 2$ leads to the 2D scattering phase shift without spin-orbital splitting, shown in figure 1 by the dash-dotted line.

Let's note that for the potential of the resonance ${}^2D_{5/2}$ wave with the FS, which will be required further for the consideration of the $E2$ transitions the following parameters were obtained

$$V_{5/2} = 474.505 \text{ MeV and } \gamma_{5/2} = 0.37 \text{ fm}^{-2}. \quad (8)$$

The potential leads to the resonance at 1.41 MeV (l.s.) at width of $\Gamma_{\text{c.m.}} = 100$ keV, that is fully consistent with the data [42], and its phase shift is shown in figure 1 by the dot-dot-dashed line.

The potential ${}^2P_{1/2}$ of the FES without the FS can have the parameters

$$V_{1/2} = 9.077594 \text{ MeV and } \gamma_{1/2} = 0.03 \text{ fm}^{-2}. \quad (9)$$

The potential leads to the binding energy of -0.181560 MeV with an accuracy of the FDM of 10^{-6} MeV [7], the AC equals 0.73(1) on the interval of 11–30 fm, the mass radius of 3.58 fm and the charge radius of 2.52 fm. The phase shift of such potential decreases gradually and at 2.0 MeV has the value, approximately, up to 115° . The potential parameters of the FES (9) were chosen for the correct description of the total cross sections of the neutron capture on ${}^{10}\text{Be}$ at thermal energy of 25.3 MeV, obtained in paper [38], and the value of its dimensionless AC is in the above allowable range of 0.29–0.81 values.

Now we return to the criteria of constructing potentials for the 2P scattering wave, which may differ from the potential of the FES because of the different Young tableaux of these states [43,44]. First of all, as was indicated above, such potential should not have the forbidden state. Therefore, we do not have the results of the phase shift analysis of the $n^{10}\text{Be}$ elastic scattering, and in the spectra of ${}^{11}\text{Be}$ at energies below 2.0 MeV there are no resonances of the negative parity, we will consider that the 2P potentials should lead in this energy range to almost zero scattering phase shifts – so they simply may have the null depth. For the potential of the ${}^2S_{1/2}$ scattering the interaction ${}^2S_{1/2}$ of the GS with the FS will be used, for instance, the variant of the potential (6), because it leads to the relatively good agreement with the scattering phase shifts from paper [59], shown by the solid line and the points in figure 1.

5. The total cross sections for the neutron radiative capture on ${}^{10}\text{Be}$

As already mentioned, we assume that the $E1$ radiation capture No. 1 comes from the 2P scattering wave to the ${}^2S_{1/2}$ GS of ${}^{11}\text{Be}$ in the $n^{10}\text{Be}$ channel. Our calculations of such capture cross sections for the potential of the GS (6) lead to the results, shown in figure 2 by the dashed line, and the results for the potential of the GS (7) are presented by the solid line. In all of these calculations for the 2P elastic scattering potentials the potential of zero depth was used. The experimental data of the neutron radiative capture on ${}^{10}\text{Be}$ are shown in figure 2 by points and are given in paper [60] with reference to the paper [61]. As seen from these results, the calculated cross sections describe the available experimental data in a relatively narrow energy range, approximately from 0.3–0.4 MeV to 2.0 MeV. The calculated line decreases rapidly at lower energies and doesn't describe the data for thermal energy, as shown in figure 3.

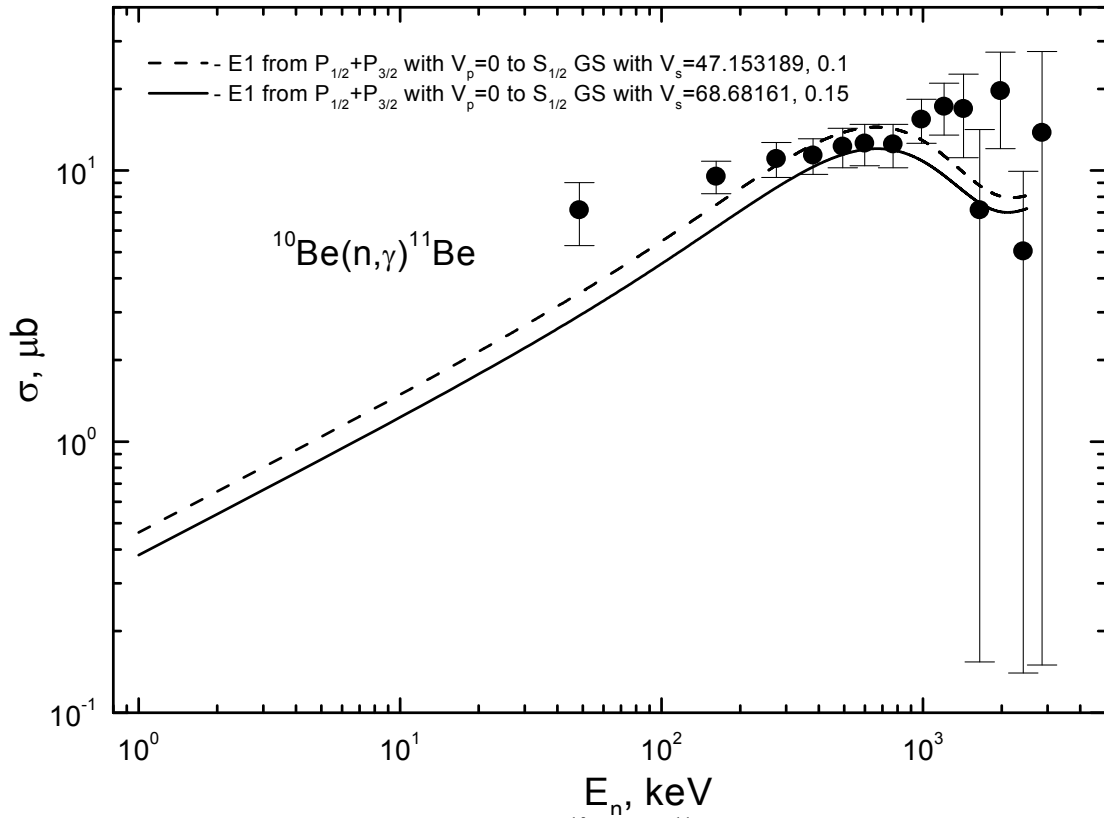


Figure 2. The total cross sections of the radiative $^{10}\text{Be}(n,\gamma)^{11}\text{Be}$ $E1$ capture to the GS. Points are the experimental data from paper [60]. The meaning of lines is explained in the text.

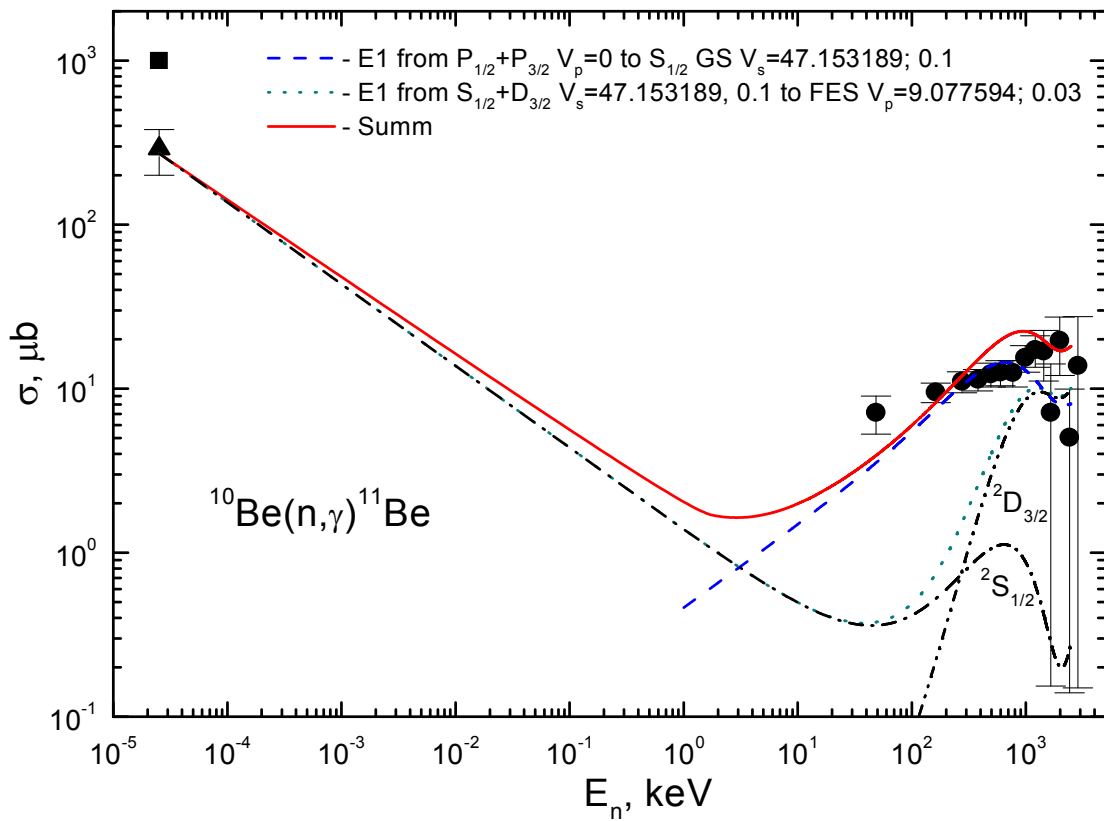


Figure 3. The total cross sections of the radiative $^{10}\text{Be}(n,\gamma)^{11}\text{Be}$ capture. The experimental data of papers: [61] – points, [38] – triangle, [62] – square. The meaning of lines is explained in the text.

Therefore, further we will consider the $E1$ transitions to the ${}^2P_{1/2}$ FES from the ${}^2S_{1/2}$ and ${}^2D_{3/2}$ scattering wave. The results for the $E1$ transition to the GS with the potential (6) and the 2P scattering potential are still shown in figure 3 by the dashed line. The cross sections for the $E1$ transition No. 2 from the ${}^2S_{1/2}+{}^2D_{3/2}$ scattering wave with the potential (6) for $L=0$ and 2 to the ${}^2P_{1/2}$ FES with the potential (9) are shown by the dotted line. The solid line shows the summarize cross section of these two $E1$ processes, which, in the large, reproduces the general course of the available experimental data correctly in the given energy region – from the thermal 25.3 meV to 2.0 MeV.

The contribution of the transition from the ${}^2S_{1/2}$ wave is shown by the dot-dashed line and from the ${}^2D_{3/2}$ scattering wave by the dot-dot-dashed line. All coefficients in the expression (3) were calculated for the ${}^2D_{3/2}$ wave, and the ${}^2S_{1/2}$ wave potential (6) used in these calculations has the orbital angular momentum $L=2$, i.e., corresponds to the 2D state without the spin-orbital. The calculated cross section at thermal energy was found to be 272 μb . The experimental data at thermal energy were taken from paper [38] – triangle with the value of 290(90) μb and [62] – the square, which indicates the upper limit of the thermal cross section equals of 1 mb.

For the comparison, now we use the potential of the GS with parameters (7). These results with the same potential of the FES (9) are shown in figure 4 (notation as in figure 3), with a cross section at thermal energy equals of 343 μb . It is evident that such potential of the GS is slightly better describes the cross section at energies from 0.1-0.2 to 2.0 MeV. Thus, the variants of the calculations with the potentials of the GS (6) and (7) and the potentials of the FES (9) lead to the general description of the available data at the energy of 25.3 meV and in the range of about 0.1–2.0 MeV. The 50–100 keV energy range is described comparatively bad, so let us consider the other variants of the transitions at the neutron capture on ${}^{10}\text{Be}$.

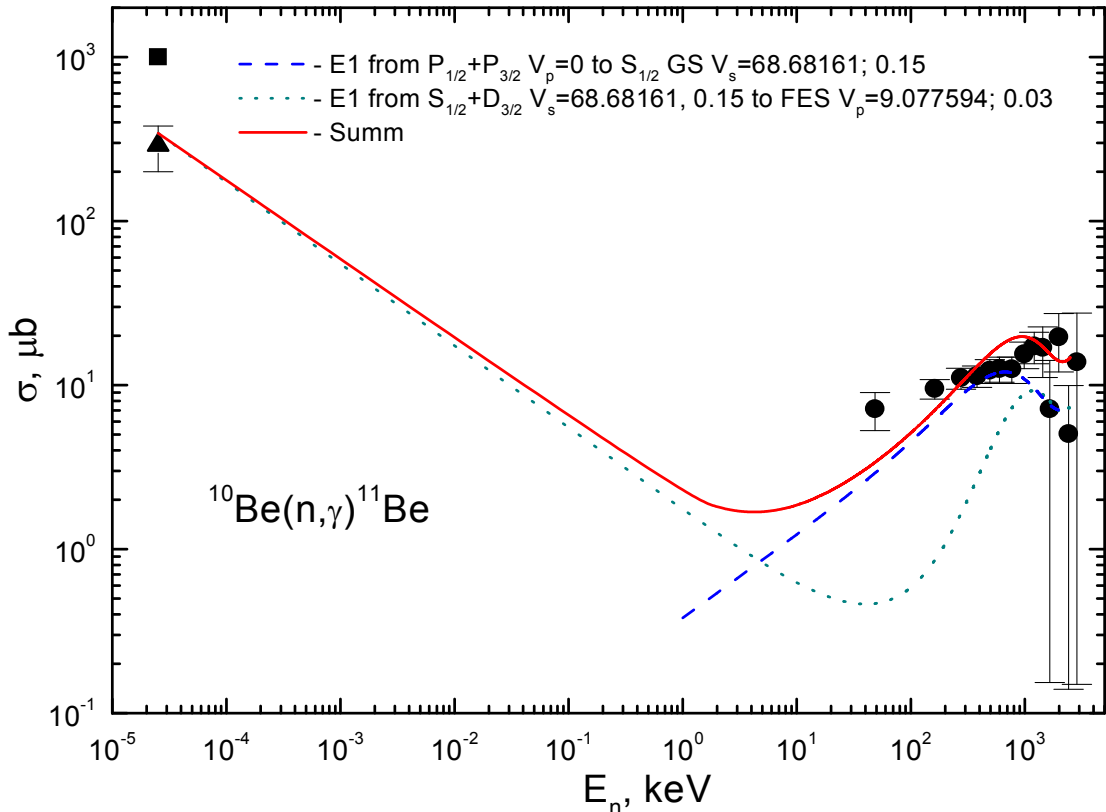


Figure 4. The total cross sections of the radiative ${}^{10}\text{Be}(n,\gamma){}^{11}\text{Be}$ capture. The experimental data of papers: [61] - points, [38] - triangle, [62] - square. The meaning of lines is explained in the text.

The cross section of the possible $M1$ transition from the ${}^2S_{1/2}$ scattering wave to the ${}^2S_{1/2}$ GS of ${}^{11}\text{Be}$ in the $n^{10}\text{Be}$ channel with the same potential (6) or (7) in the both states will tend to zero because of the orthogonality of the wave functions of discrete and continuous spectra in the same potential. The actual numerical calculation of these cross sections leads to a value less than 10^{-2} μb in the energy range from 1 keV to 2.0 MeV, and at the energy of 25.3 meV the cross section occurs to be slightly less than 1% from the cross section of the transition to the FES, shown in figure 4 by the dotted line.

If we consider the $M1$ transitions from the 2P scattering waves with the zero potential to the ${}^2P_{1/2}$ FES with the potential (9), then the sections don't exceed 0.15 μb in the entire energy region. For the $E2$ transitions from the ${}^2D_{3/2}$ wave with the potential (6) or (7) at $L = 2$ and the ${}^2D_{5/2}$ wave with the potential (8) to the GS with the ${}^2S_{1/2}$ even at the resonance energies the value of these cross sections do not exceed 10^{-3} μb . Hence, it is clear that such transitions are not contribute significantly to the total cross section of the considered process and the problem of description of the cross sections in the range from 50 keV to 100–200 keV remains open.

Since at energies of 25.3 meV and up to about 10 eV, the calculated cross section is a straight line (solid line in figure 4), it can be approximated by a simple function of energy of the form [34]

$$\sigma_{\text{ap}} (\mu\text{b}) = \frac{A}{\sqrt{E_n (\text{keV})}}. \quad (10)$$

The value of the constant $A = 1.7265 \mu\text{b}\cdot\text{keV}^{1/2}$ was determined by a single point in the calculated cross section at minimum energy equals of 25.3 meV. The module of the relative deviation

$$M(E) = \left| [\sigma_{\text{ap}}(E) - \sigma_{\text{theor}}(E)] / \sigma_{\text{theor}}(E) \right| \quad (11)$$

of the calculated theoretical cross section (σ_{theor}) and approximation (σ_{ap}) of this cross section of the given above function (10) in the energy range up to 10 eV is located at the level of 0.1%.

It is realistic to assume that this form of dependence of the total cross section from energy will also be saved at lower energies. Therefore, based on the given expression (10) for approximation of the cross section one can perform the estimation of the cross section, for instance, at energy of 1 μeV (1 $\mu\text{eV} = 10^{-9}$ keV), which gives a value of about 54.6 mb.

6. Conclusion

Thus, in the frame of the MPCM with the classification of states according to Young tableaux is quite possible to construct the potentials of the $n^{10}\text{Be}$ interaction, which allow one to reproduce the general course of the experimental data for the total cross sections of the radiative neutron capture on ${}^{10}\text{Be}$ at low and ultralow energies generally correct. The theoretical cross sections are calculated from thermal energy 25.3 meV to 2.0 MeV and approximated by a simple function of energy, which can be used to calculate the cross sections at energies below 10–50 eV.

The proposed variants of the potentials of the ground and the first excited states of ^{11}Be in the $n^{10}\text{Be}$ channel allow to obtain the AC within available for it errors, and lead to a reasonable description of the ^{11}Be radius. The result shows that in the 29th cluster system of light nuclei in the framework of the single-channel MPCM it is possible to describe some of the main characteristics of the nucleus and, in general, the total cross section of the neutron radiative capture on ^{10}Be correctly.

Acknowledgments

This work was supported in the framework of the grant program “Studying of the thermonuclear processes in the Universe” of the Ministry of Education and Science of the Republic of Kazakhstan through the V.G. Fessenkov Astrophysical Institute, “NCSRT” ASC MID RK.

In conclusion, the authors express their deep gratitude to Strakovsky I.I. (GWU, Washington, USA) and Uzikov Y.N. (JINR, Dubna, Russia) for a discussion of certain issues touched in the paper.

References

1. Dubovichenko S B and Dzhazairov-Kakhramanov A V 1994 Calculation of coulomb form-factors of lithium nuclei in a cluster model based on potentials with forbidden states *Phys. Atom. Nucl.* **57** 733-40
2. Dubovichenko S B and Dzhazairov-Kakhramanov A V 1997 Electromagnetic effects in light nuclei and the cluster potential model *Phys. Part. Nucl.* **28** 615-41
3. Dubovichenko S B 2012 *Thermonuclear processes of the Universe* (New-York: NOVA Scientific Publishing); https://www.novapublishers.com/catalog/product_info.php?products_id=31125
4. Dubovichenko S B, Neudatchin V G, Sakharuk A A and Smirnov Yu F 1990 Generalized potential description of the interaction of the lightest nuclei $p^3\text{H}$ and $p^3\text{He}$ *Izv. Akad. Nauk SSSR Ser. Fiz.* **54** 911-6
5. Neudatchin V G, Sakharuk A A and Dubovichenko S B 1995 Photodisintegration of ^4He and the supermultiplet potential model of cluster-cluster interactions *Few-Body Systems* **18** 159-72
6. Dubovichenko S B 2013 *Light nuclei and nuclear astrophysics*. Sec. edition, revised and expanded. (Saarbrücken: Lambert Acad. Publ. GmbH&Co. KG); [https://www.lap-publishing.com/catalog/details/store/fr/book/978-3-659-41308-7/Light nuclei and nuclear astrophysics \(in Russian\)](https://www.lap-publishing.com/catalog/details/store/fr/book/978-3-659-41308-7/Light%20nuclei%20and%20nuclear%20astrophysics%20(in%20Russian)).
7. Dubovichenko S B 2012 *Calculation methods of nuclear characteristics* Sec. edition, revised and expanded. (Saarbrücken: Lambert Acad. Publ. GmbH&Co. KG.); <https://www.lap-publishing.com/catalog/details/store/ru/book/978-3-659-21137-9/metody-rascheta-yadernyh-kharacteristic> (in Russian).
8. Dubovichenko S B and Dzhazairov-Kakhramanov A V 1990 Potential description of elastic N^2H , $^2\text{H}^2\text{H}$, N^4He and $^2\text{H}^3\text{He}$ scattering *Sov. Jour. Nucl. Phys.* **51** 971-7
9. Dubovichenko S B 1995 Analysis of photonuclear processes in the N^2H and $^2\text{H}^3\text{He}$ systems on the basis of cluster-models for potentials with forbidden states *Phys. Atom. Nucl.* **58** 1174-80

10. Dubovichenko S B and Zhusupov M A 1984 The structure of light-nuclei with $A=6,7,8$ in cluster models for potentials with forbidden states *Izv. Akad. Nauk SSSR Ser. Fiz.* **48** 935-7
11. Dubovichenko S B and Zhusupov M A 1984 Some characteristics of the nucleus ${}^7\text{Li}$ in the ${}^3\text{H}^4\text{He}$ model for potentials with forbidden states *Sov. Jour. Nucl. Phys.* **39** 870-2
12. Dubovichenko S B 1998 Tensor ${}^2\text{H}^4\text{He}$ interactions in the potential cluster model involving forbidden states *Phys. Atom. Nucl.* **61** 162-8
13. Kukulín V I, Pomerantsev V N, Cooper S G and Dubovichenko S B 1998 Improved $d^4\text{He}$ potentials by inversion: The tensor force and validity of the double folding model *Phys. Rev. C* **57** 2462-73
14. Dubovichenko S B and Dzhazairov-Kakhramanov A V 2009 Astrophysical S -factor of the radiative $p^2\text{H}$ capture *Euro. Phys. Jour. A* **39** 139-43
15. Dubovichenko S B and Burkova N A 2014 Radiative $n^{11}\text{B}$ capture at astrophysical energies *Mod. Phys. Lett. A* **29** 1450036(1-14)
16. Dubovichenko S B, Dzhazairov-Kakhramanov A V, Burtebaev N and Alimov D 2014 Radiative $p^{14}\text{C}$ capture at astrophysical energies *Mod. Phys. Lett. A* **29** 1450125(1-16)
17. Dubovichenko S B and Dzhazairov-Kakhramanov A V 2012 Radiative $n^7\text{Li}$ capture at Astrophysical Energies *Annalen der Physik* **524** 850-61
18. Dubovichenko S B 2010 Astrophysical S -factors of radiative ${}^3\text{He}^4\text{He}$, ${}^3\text{H}^4\text{He}$, and ${}^2\text{H}^4\text{He}$ capture *Phys. Atom. Nucl.* **73** 1526-38
19. Dubovichenko S B 2011 Astrophysical S -factors for radiative proton capture by ${}^3\text{H}$ and ${}^7\text{Li}$ nuclei *Phys. Atom. Nucl.* **74** 358-70
20. Dubovichenko S B 2012 Astrophysical S -factor for the radiative-capture reaction $p^{13}\text{C} \rightarrow {}^{14}\text{N}\gamma$ *Phys. Atom. Nucl.* **75** 173-81
21. Dubovichenko S B 2013 Radiative neutron capture by ${}^2\text{H}$, ${}^7\text{Li}$, ${}^{14}\text{C}$, and ${}^{14}\text{N}$ nuclei at astrophysical energies *Phys. Atom. Nucl.* **76** 841-61
22. Dubovichenko S B 2013 Capture of a neutron to excited states of $n^9\text{Be}$ nucleus taking into account resonance at 622 keV *Jour. Experim. and Theor. Phys.* **117** 649-55
23. Dubovichenko S B 2012 Radiative $n^2\text{H}$ capture at low energies *Rus. Phys. Jour.* **55** 138-45
24. Dubovichenko S B 2011 Contribution of the M1 process to the astrophysical S -factor of the $p^2\text{H}$ radiative capture *Rus. Phys. Jour.* **54** 157-64
25. Dubovichenko S B and Dzhazairov-Kakhramanov A V 2009 Astrophysical S -factor for $p^{12}\text{C} \rightarrow {}^{13}\text{N}\gamma$ radiative capture *Rus. Phys. Jour.* **52** 833-40
26. Dubovichenko S B and Uzikov Yu N 2011 Astrophysical S -factors of reactions with light nuclei *Phys. Part. Nucl.* **42** 251-301
27. Dubovichenko S B 2013 Neutron capture by light nuclei at astrophysical energies *Phys. Part. Nucl.* **44** 803-47.
28. Dubovichenko S B and Dzhazairov-Kakhramanov A V 2012 Examination of astrophysical S -factors of $p^2\text{H}$, $p^6\text{Li}$, $p^7\text{Li}$, $p^{12}\text{C}$ and $p^{13}\text{C}$ radiative capture reactions *Int. Jour. Mod. Phys. E* **21** 1250039(1-44)
29. Dubovichenko S B, Dzhazairov-Kakhramanov A V and Afanasyeva N V 2013 Radiative neutron capture on ${}^9\text{Be}$, ${}^{14}\text{C}$, ${}^{14}\text{N}$, ${}^{15}\text{N}$ and ${}^{16}\text{O}$ at thermal and astrophysical energies *Int. Jour. Mod. Phys. E* **22** 1350075(1-53)
30. Dubovichenko S B, Dzhazairov-Kakhramanov A V and Burkova N A 2013 The

- radiative neutron capture on ^2H , ^6Li , ^7Li , ^{12}C and ^{13}C at astrophysical energies *Int. Jour. Mod. Phys. E* **22** 1350028(1-52)
31. Dubovichenko S B and Dzhazairov-Kakhramanov A V 2014 Neutron radiative capture by ^{10}B , ^{11}B and proton radiative capture by ^{11}B , ^{14}C and ^{15}N at thermal and astrophysical energies *Int. Jour. Mod. Phys. E* **23** 1430012(1-55)
 32. Dubovichenko S B and Dzhazairov-Kakhramanov A V 2013 Neutron radiative capture by ^2H , ^6Li , ^7Li , ^{12}C , ^{13}C , ^{14}C and ^{14}N at astrophysical energies In: *The Universe Evolution. Astrophysical and Nuclear Aspects* (New-York: NOVA Sci. Publ.) P.49-108
 33. Dubovichenko S B and Dzhazairov-Kakhramanov A V 2012. Astrophysical S -factors of proton radiative capture in thermonuclear reactions in the Stars and the Universe In: *The Big Bang: Theory, Assumptions and Problems* (New-York: NOVA Sci. Publ.) P.1-60
 34. Dubovichenko S B 2014 *Primordial nucleosynthesis of the Universe*. Fourth edition, revised and expanded. (Saarbrucken: Lambert Acad. Publ. GmbH&Co. KG) 668p.; [https://www.lap-publishing.com/catalog/details/store/fr/book/978-3-659-54311-1/Primordial nucleosynthesis of the Universe \(in Russian\)](https://www.lap-publishing.com/catalog/details/store/fr/book/978-3-659-54311-1/Primordial%20nucleosynthesis%20of%20the%20Universe%20(in%20Russian).).
 35. Neudatchin V G and Smirnov Yu F 1969 *Nucleon associations in light nuclei* (Moscow: Nauka) 414p. (in Russian)
 36. Angulo C *et al* 1999 A compilation of charged-particle induced thermonuclear reaction rates *Nucl. Phys. A* **656** 3-183
 37. Adelberger E G *et al* 2011 Solar fusion cross sections. II. The pp chain and CNO cycles *Rev. Mod. Phys.* **83** 195-245
 38. Liu Zu-Hua and Zhou Hong-Yu 2005 Nuclear halo effect on nucleon capture reaction rate at stellar energies // *Chi. Phys.* **14** 1544-8
 39. Guimaraes V *et al* 2006 Investigation of nucleosynthesis neutron capture reactions using transfer reactions induced by ^8Li beam *International Symposium on Nuclear Astrophysics - Nuclei in the Cosmos IX* June 25-30 (Switzerland, Geneva: CERN) P.108
 40. Itzykson C and Nauenberg M 1966 Unitary groups: Representations and decompositions *Rev. Mod. Phys.* **38** 95-101
 41. Tilley D R *et al* 2004 Energy level of light nuclei $A=8,9,10$ *Nucl. Phys. A* **745** 155-362
 42. Kelley J H *et al* 2012 Energy level of light nuclei $A=11$ *Nucl. Phys. A* **880** 88-195
 43. Neudatchin V G, Sakharuk A A and Smirnov Yu F 1992 Generalized potential description of interaction of the lightest cluster scattering and photonuclear reactions *Sov. J. Part. Nucl.* **23** 210-71
 44. Neudatchin V G, Struzhko B G and Lebedev V M 2005 Supermultiplet potential model of the interaction of light clusters and unified description of various nuclear reactions *Phys. Part. Nucl.* **36** 468-519
 45. Plattner G R and Viollier R D 1981 Coupling constants of commonly used nuclear probes *Nucl. Phys. A* **365** 8-12
 46. Nörtershäuser W *et al* 2009 Nuclear Charge Radii of $^{7,9,10}\text{Be}$ and the One-Neutron Halo Nucleus ^{11}Be *Phys. Rev. Lett.* **102** 062503
 47. Hammer H W and Phillips D R 2011 Electric properties of the Beryllium-11 system in Halo EFT *Nuclear Physics A* **865** 17-42
 48. Belyaeva T L *et al* 2014 Neutron asymptotic normalization coefficients and halo

- radii of the first excited states of ^{12}C and ^{11}Be *EPJ Web of Conferences* **66** 03009
49. http://cdf.e.sinp.msu.ru/services/ground/NuclChart_release.html
 50. http://physics.nist.gov/cgi-bin/cuu/Value?mud|search_for=atomnuc!
 51. Navin A *et al* 2000 Direct Evidence for the Breakdown of the $N=8$ Shell Closure in ^{12}Be *Phys. Rev. Lett.* **85** 266
 52. Fukuda N *et al* 2004 Coulomb and nuclear breakup of a halo nucleus ^{11}Be *Phys. Rev. C* **70** 054606
 53. Palit R. *et al* 2003 Exclusive measurement of breakup reactions with the one-neutron halo nucleus ^{11}Be *Phys. Rev. C* **68** 034318
 54. Pain S D *et al* 2005 Experimental evidence of a $(1d_{5/2})^2$ component to the ^{12}Be ground state *Eur. Phys. J. A* **25** Suppl.1 349-51
 55. Pain S D *et al* 2006 Structure of ^{12}Be : Intruder d -Wave Strength at $N=8$ *Phys. Rev. Lett.* **96** 032502
 56. Auton D L 1970 Direct reactions on ^{10}Be *Nucl. Phys. A* **157** 305-22
 57. Goosman D R and Kavanagh R W 1970 $^{10}\text{Be}(d, p)^{11}\text{Be}$ and the $^{10}\text{Be}(d, \alpha)^8\text{Li}$ Reactions *Phys. Rev. C* **1** 1939
 58. Zwiaglinski B. *et al* 1979 Study of the $^{10}\text{Be}(d, p)^{11}\text{Be}$ reaction at 25 MeV *Nucl. Phys. A* **315** 124-32
 59. Quaglioni S. and Navrátil P. 2009 Ab initio many-body calculations of nucleon-nucleus scattering *Phys. Rev. C* **79** 044606
 60. Mengoni A *et al* 1996 *Exotic properties of light nuclei and their neutron capture cross sections* 4th International Seminar on Interaction of Neutrons with Nuclei "Neutron Spectroscopy, Nuclear Structure, Related Topics" Dubna (Russia), April 1996 (arXiv:nucl-th/9607023)
 61. Nakamura T *et al* 1994 Coulomb dissociation of a halo nucleus ^{11}Be at 72 MeV *Phys. Lett. B* **331** 296-301
 62. Mughabghab S F 2006 *Atlas of neutron resonances. National Nuclear Data Center* (Brookhaven. National Laboratory. Upton, USA) 1008p.